
This is an electronic reprint of the original article.
This reprint may differ from the original in pagination and typographic detail.

Järvinen, Ellen; Velasco, Jorge A.; Karinen, Reetta; Puurunen, Riikka L.

Characterization of Unmodified and Zinc-modified ZSM-5 Zeolites with Temperature-programmed Desorption of Ammonia and Isopropylamine

Published in:
Topics in Catalysis

DOI:
[10.1007/s11244-025-02112-0](https://doi.org/10.1007/s11244-025-02112-0)

Published: 01/12/2025

Document Version
Publisher's PDF, also known as Version of record

Published under the following license:
CC BY

Please cite the original version:
Järvinen, E., Velasco, J. A., Karinen, R., & Puurunen, R. L. (2025). Characterization of Unmodified and Zinc-modified ZSM-5 Zeolites with Temperature-programmed Desorption of Ammonia and Isopropylamine. *Topics in Catalysis*, 68(20), 2393-2403. <https://doi.org/10.1007/s11244-025-02112-0>

This material is protected by copyright and other intellectual property rights, and duplication or sale of all or part of any of the repository collections is not permitted, except that material may be duplicated by you for your research use or educational purposes in electronic or print form. You must obtain permission for any other use. Electronic or print copies may not be offered, whether for sale or otherwise to anyone who is not an authorised user.



Characterization of Unmodified and Zinc-modified ZSM-5 Zeolites with Temperature-programmed Desorption of Ammonia and Isopropylamine

Ellen Järvinen¹ · Jorge A. Velasco¹ · Reetta Karinen¹ · Riikka L. Puurunen¹

Accepted: 15 May 2025 / Published online: 10 June 2025
© The Author(s) 2025

Abstract

While the temperature-programmed desorption of ammonia (NH₃-TPD) is widely used to analyze the combined Lewis and Brønsted acidity of heterogeneous catalysts, the temperature-programmed desorption of isopropylamine (IPAm-TPD) can be used for the selective analysis of Brønsted acidity. This work compared NH₃-TPD and IPAm-TPD as analysis methods for the acidity of zeolitic samples, including H-ZSM-5-23, H-ZSM-5-50, H-ZSM-5-280, a Zn-modified H-ZSM-5-50 sample, and a γ -Al₂O₃ reference sample. For the unmodified H-ZSM-5-23, H-ZSM-5-50, and H-ZSM-5-280, the total acidity determined with NH₃-TPD remained higher and the Brønsted acidity determined with IPAm-TPD lower than the theoretical acidity estimated with the Al content of the materials. When the NH₃-TPD saturation temperature was varied for H-ZSM-5-50 to examine the trends observed in the analyses, the temperature change affected primarily the low temperature peak of the TPD traces. The Zn-modified Zn/H-ZSM-5-50 sample yielded a multi-peak IPAm-TPD trace, though only a single peak trace was expected. Additionally, the value of Brønsted acidity showed no change from the unmodified zeolite.

Keywords Acidity · NH₃-TPD · IPAm-TPD · H-ZSM-5

1 Introduction

Surface acid sites are a major source of catalytic activity with certain solid heterogeneous catalysts such as zeolites. Analysis methods that can quantify the surface acidity of such materials are important in catalysis research, as they can explain the relationship between the catalytic activity and the surface chemical properties of the catalysts. The temperature-programmed desorption (TPD) of basic probe molecules is a widely used acidity characterization method based on the adsorption of gases onto the acidic sites of the sample material [1]. Commercially available TPD instruments that require little operator input to perform the

analysis make TPD methods accessible for routine acidity characterization [2].

Various bases have been reported as probe molecules for TPD acidity characterization, including NH₃ and alkylamines such as isopropylamine (IPAm) [3]. Several works from various authors have examined NH₃ adsorption for acidity characterization [4–12], and an ASTM standard (ASTM D4824-24) exists for the surface acidity characterization with NH₃ chemisorption [13]. In turn, the pioneering work in surface acidity analysis by IPAm-TPD was published by Gorte and coworkers first in the 1980s and 1990s [14–24]. At present, numerous studies employ NH₃-TPD for acidity characterization, while IPAm-TPD has been less frequently used. To illustrate the difference in prevalence, NH₃-TPD is mentioned in over 200 times more works in the Web of Science database compared to IPAm-TPD, when examining literature from the last 20 years [25, 26].

The working principles of NH₃-TPD and IPAm-TPD differ somewhat. In both methods, the sample is saturated with the probe molecule, the weakly adsorbed molecules are purged using inert gas, and the sample is heated at a

✉ Ellen Järvinen
ellen.jarvinen@aalto.fi

¹ Department of Chemical and Metallurgical Engineering, School of Chemical Engineering, Aalto University, P.O. Box 16100, Aalto 00076, Finland

constant rate to observe the desorption of the probe molecule. The difference is related to the surface chemical reactions during the heating program and is illustrated Fig. 1. In NH_3 -TPD, the NH_3 molecules adsorb and desorb without reacting [27]. By contrast, IPAm decomposes on Brønsted sites into propylene and NH_3 [18]. When the decomposition products are followed with a detector capable of identifying the individual species in the gas stream, such as a mass spectrometer (MS), the Brønsted acidity can be selectively quantified.

Both analyses have reportedly been performed at similar conditions for zeolitic samples. For NH_3 -TPD, the samples have been reported to be saturated in a constant flow of a NH_3/He gas mixture at 100–150 °C and heated at 5–15 °C/min up to 500–650 °C [4, 28–35]. For IPAm-TPD, the samples have been reported to be saturated by pulse chemisorption at 100–125 °C and heated at 5–10 °C/min up to 400–800 °C [30, 33, 35–38], though even ambient temperature has been used for the saturation [39]. For comparison, the application notes of Micromeritics, a manufacturer of thermochemical characterization instruments, instruct a saturation temperature of 120 °C and a 10 °C/min temperature ramp up to 500 °C for NH_3 -TPD [40]. The conditions indicated for IPAm-TPD are 200 °C and a 10 °C/min temperature ramp up to 500 °C [41].

In terms of typical results obtained with NH_3 -TPD and IPAm-TPD, NH_3 -TPD traces of zeolites commonly exhibit a distinct low temperature and high temperature peak [42]. The low temperature peak is generally observed at 170–280 °C and the high temperature peak at 370–440 °C [8]. The NH_3 -TPD high temperature peak is commonly attributed to strong Brønsted and Lewis acid sites [8], while the low temperature peak has been linked to other weaker adsorption sites [42]. In contrast, the IPAm-TPD traces typically exhibit a single peak associated with IPAm decomposition at approximately 300–375 °C [17, 43].

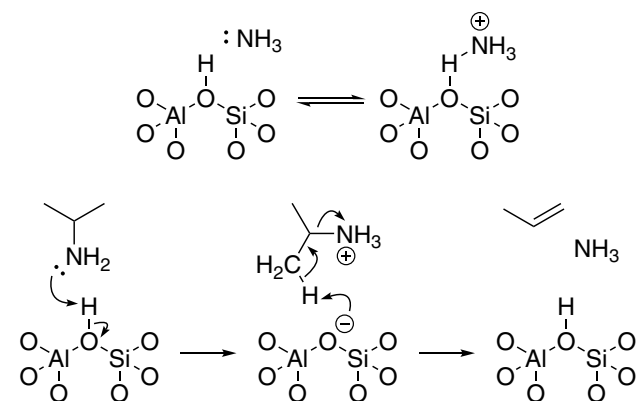


Fig. 1 Reaction schemes of the interaction of NH_3 and IPAm on a zeolite bridging Brønsted site

Regarding typical quantitative results of zeolitic samples, the observed amount of acidic sites for the same material may be influenced strongly by operating parameters, which can lead to vast differences in values reported in different works [18]. For example, both the value 690 $\mu\text{mol/g}$ [34] and 1464 $\mu\text{mol/g}$ [28] has been reportedly obtained with NH_3 -TPD from a commercial H-ZSM-5-23 material. Similarly, the IPAm-TPD-based Brønsted acidity reported for commercial H-ZSM-5-23 was 435 $\mu\text{mol/g}$ in one study [39], while another study reported a Brønsted acidity of 1260 $\mu\text{mol/g}$ for a H-ZSM-5-25 material [38]. To provide a stable comparison point for the measured acidities, some works have estimated the theoretical acidity of the materials with elemental content [8, 44]. For example, the Brønsted acidity is heavily related to the amount of Al in aluminosilicate zeolites, and in ideal zeolites with perfect crystallinity, each Brønsted site is associated with an Al atom [8].

This work aimed to examine NH_3 -TPD and IPAm-TPD as analysis methods for zeolite acidity and presents our initial comparison of the acidic properties of selected zeolitic samples as analyzed by NH_3 -TPD and IPAm-TPD. The analysis results from both methods were compared by performing NH_3 -TPD and IPAm-TPD for H-ZSM-5 samples with selected $\text{SiO}_2/\text{Al}_2\text{O}_3$ ratios as well as a $\gamma\text{-Al}_2\text{O}_3$ reference sample. The Al content of the zeolites determined with elemental analysis was used as an estimate for the theoretical acidity to facilitate the comparison. As NH_3 -TPD and IPAm-TPD differ in selectivity towards different types of acidic sites, this work also examined the acidity of a zeolite before and after the addition of Zn by comparing the NH_3 -TPD and IPAm-TPD results of an unmodified H-ZSM-5-50 sample and a Zn-modified Zn/H-ZSM-5-50 sample.

2 Experimental

Materials.

The TPD analysis was made for commercial ammonium-form NH_4 -ZSM-5-23 (Thermo Scientific Chemicals, prod. 45879, 425 m^2/g), NH_4 -ZSM-5-50 (Thermo Scientific Chemicals, prod. 45881, 425 m^2/g), NH_4 -ZSM-5-280 (Zeolyst International, prod. CBV28014, 400 m^2/g), and $\gamma\text{-Al}_2\text{O}_3$ (Alfa Aesar, prod. 39812, 99.97%, 80 m^2/g). Zn(II) acetylacetonate ($\text{Zn}(\text{acac})_2$, Volatec, CAS: 14024-63-6, 99.99%) and synthetic air (Woikoski, prod. N50, 99.999%) were used as the ALD reactants in the Zn-modification of ZSM-5-50. A 10 vol-% NH_3/He gas mixture (Air Products, prod. 305434, 10.01 \pm 1% NH_3 , 89.99 \pm 1% He), pure He (Woikoski, prod. N46, 99.996%), high-purity propylene (Sigma-Aldrich, prod. 295663, CAS: 115-07-1, \geq 99%), and GC-grade isopropylamine (Sigma-Aldrich, prod. 59330, CAS: 75-31-0, \geq 97.0%) were used in the TPD analyses.

Sample preparation.

To obtain the proton-form H-ZSM-5-23, H-ZSM-5-50, and H-ZSM-5-280, the ammonium-form commercial zeolites were de-ammoniated in a muffle furnace in static ambient air. The samples were first heated from ambient temperature to 200 °C for 1 h and held at 200 °C for 50 min, then heated from 200 °C to 400 °C for 1 h 10 min and held at 400 °C for 4 h. The Al₂O₃ was calcined in a muffle furnace in static ambient air at 600 °C for 10 h before analysis.

The ZSM-5-50 zeolite used as a support for the Zn-modification was pressed and sieved prior to treatment with atomic layer deposition (ALD). Ammonium-form NH₄-ZSM-5-50 was pelletized with a Unipress Equipment U111 High Pressure Multivessel Apparatus. About 1.5 g of the material was placed into the sample chamber in a silicone tube and pressurized to 1200 bar. The pressure was maintained for 5 min. The formed pellet was crushed and sieved to obtain 150–250 μm particles and subsequently de-ammoniated.

To obtain a Zn-modified H-ZSM-5-50 sample, H-ZSM-5-50 was treated with one cycle of ALD using the procedure described by Yim et al. [45]. A flow-type fixed bed F-120 ALD reactor (ASM Microchemistry) was used. About 2 g of the zeolite (150–250 μm) was pre-treated for 5 h at 250 °C to remove any adsorbed moisture. About 2.4 g of solid Zn(acac)₂ was evaporated at 120 °C at about 6 mbar in 100 sccm N₂ flow and delivered to the H-ZSM-5-50 sample at 200 °C for 3 h. After Zn delivery and cooling to ambient conditions, the top and bottom parts of the Zn-modified zeolite particle bed were separated, and only the top part was analyzed. The top part was transferred through air to a flow-through furnace and calcined at 550 °C in 100 sccm synthetic airflow for 10 h to remove remaining acetylacetonate ligands from the sample.

X-ray fluorescence elemental analysis.

The elemental analysis was performed with X-ray fluorescence (XRF) using borate fusion for analysis sample preparation. About 0.2–0.5 g of sample material was fused with 10 g of a 50.0% lithium tetraborate and 50.0% lithium metaborate flux (XRF Scientific, 99.995%, 0.5% LiI additive) with a Katanax X-300 automated fusion instrument (see Table S1). The resulting beads were analyzed with a Malvern Panalytical Axios mAX 3 kW instrument (Rh source, 60 kV, 125 mA) in vacuum using 27 mm diameter sample holders.

The standardless Omnian method was used to quantify the elemental content [46], which yielded the amount of an element and its oxide in mass percentages. The mass percentage of Zn obtained with Omnian was regarded as the Zn loading of the zeolite sample. The Al content C_{Al} (mol/g) was calculated with Eq. (1),

$$C_{Al} = 2 \cdot \frac{x_{Al_2O_3}}{M_{Al_2O_3}}$$

(1)

where $x_{Al_2O_3}$ is the mass fraction of Al₂O₃ in the sample derived from the Omnian mass percentage of Al₂O₃, and $M_{Al_2O_3}$ is the molar mass of Al₂O₃ (g/mol).

Temperature-programmed desorption of ammonia.

A Micromeritics AutoChem III 2930 instrument equipped with a Cirrus 3 mass spectrometer was used for the NH₃-TPD analyses. The samples were dried for several hours at 110 °C in static ambient air before analysis. About 0.05–0.1 g of the dried sample was placed in a quartz sample cell between two pieces of quartz wool (Micromeritics, prod. 004-32164-01).

The NH₃-TPD operating parameters followed recommendations from the analysis instrument manufacturer [40], though a higher temperature was used for the pre-treatment and desorption heating ramp maximum. The sample was pre-treated in 50 sccm He flow by heating to 550 °C at 10 °C/min and maintaining 550 °C for 1 h. The sample was then cooled to a saturation temperature of 120 °C and exposed to a 50 sccm flow of 10 vol-% NH₃/He for 1 h. After the exposure, the sample was purged with He for 1 h to remove weakly adsorbed NH₃. The sample was then heated from 120 °C to 550 °C at 10 °C/min under 50 sccm He flow and held at 550 °C for 30 min, while the desorption of NH₃ was monitored with the MS following m/z 17 for NH₃.

To further examine trends that were observed in the TPD analyses, the saturation temperature was varied while otherwise maintaining the same analysis conditions as in the other analyses. NH₃-TPD was performed with a H-ZSM-5-50 sample with the saturation temperatures 50, 100, 120, 150, and 200 °C.

To determine the amount of total acid sites (mol/g), the m/z 17 signal recorded during the desorption step of each analysis run was integrated using the AutoChem III software. For the analyses performed at different saturation temperatures, the peaks of the TPD traces were integrated separately with Gaussian fits to the data. A calibration was performed for each experiment with five about 0.5 cm³ loop injections (calibrated loop volume 0.5185 cm³, loop temperature 110 °C) of the 10% NH₃/He gas mixture while following the m/z 17 signal with the MS for NH₃. The average of area of the calibration peaks was determined by integration with the AutoChem III software. The total acidity A_{tot} (mol/g) was calculated with Eq. (2)

$$A_{tot} = \frac{V_{cal} \cdot I}{I_{cal}} \cdot \frac{1}{V_m \cdot m}$$

(2)

where I is the integrated area of the m/z 17 signal peaks, I_{cal} is the average area of the calibration m/z 17 signal peaks (Table S2), V_{cal} is the loop gas volume (cm^3 STP) (Table S2), V_m is the molar volume of ideal gas (cm^3 STP/mol), and m is the sample mass (g).

Temperature-programmed desorption of isopropylamine.

The same Micromeritics AutoChem III 2930 instrument and Cirrus 3 MS, as well as the same pre-analysis drying procedure and sample loading method was used for the IPAm-TPD analyses as for the NH_3 -TPD analyses. The IPAm-TPD operating parameters followed recommendations from the analysis instrument manufacturer [41]. The

sample was pre-treated in 50 sccm He flow by heating to 500 °C at 10 °C/min and maintaining 500 °C for 1 h. The sample was then cooled to 200 °C and saturated with IPAm pulse chemisorption, where 10 of about 0.5 cm^3 loop injections (calibrated loop volume 0.5185 cm^3 , loop temperature 110 °C) were delivered. For the pulse chemisorption, the IPAm was vaporized and delivered to the injection loop by bubbling 10 sccm He through the liquid IPAm (liquid flask temperature 30 °C, reflux condenser temperature 25 °C). The saturated sample was purged with 50 sccm He for 30 min to remove weakly adsorbed IPAm. The sample was then heated from 200 °C to 500 °C at 10 °C/min under 50 sccm He flow and held at 500 °C for 30 min, while the desorption of IPAm, propylene, and NH_3 was monitored with the MS following m/z 44, 41, and 17, respectively.

To determine the amount of Brønsted acid sites, the m/z 41 signal of propylene recorded during the desorption step of each analysis run was integrated using the AutoChem III software. A calibration was performed for each experiment with 0.2, 0.4, 0.6, 0.8, and 1.0 cm^3 manual injections of propylene while following the m/z 41 signal. The area of the calibration peaks was determined by integration with the AutoChem III software, and linear regression was used to determine the slope and intercept of the calibration curve. The Brønsted acidity A_B (mol/g) was calculated with Eq. (3)

$$A_B = (kI + b) \cdot \frac{1}{V_m \cdot m}$$

(3)

where I is the integrated area of the m/z 41 signal, k is the slope (cm^3 STP/peak area) (Table S3) and b the intercept (cm^3 STP/peak area) of the calibration curve (Table S3), V_m is the molar volume of ideal gas (cm^3 STP/mol), and m is the sample mass (g).

3 Results

Acidity of samples with varying theoretical acidities.

The amount of total acid sites and Brønsted acid sites of H-ZSM-5-23, H-ZSM-5-50, H-ZSM-5-280, and $\gamma\text{-Al}_2\text{O}_3$ were analyzed with NH_3 -TPD and IPAm-TPD, respectively. Figure 2a displays the measured NH_3 -TPD traces. As shown in the figure, the overall intensity of the signals increased in the order $\gamma\text{-Al}_2\text{O}_3 < \text{H-ZSM-5-280} < \text{H-ZSM-5-50} < \text{H-ZSM-5-23}$. The NH_3 -TPD traces of the zeolites each contained a low temperature and a high temperature peak. The low temperature peaks were centered at approximately 190–230 °C and the high temperature peaks at 370–430 °C. In contrast, the $\gamma\text{-Al}_2\text{O}_3$ trace only showed a single peak centered at 245 °C.

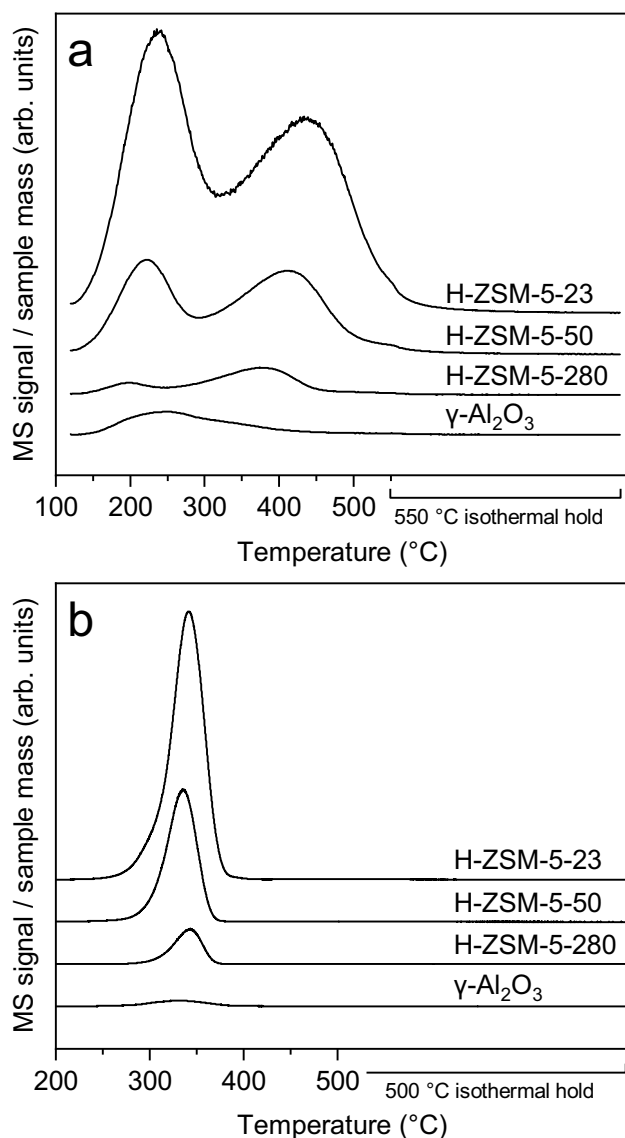


Fig. 2 The desorption traces recorded for H-ZSM-5-23, H-ZSM-5-50, H-ZSM-5-280, and $\gamma\text{-Al}_2\text{O}_3$ during (a) NH_3 -TPD (desorption 120–550 °C, 10 °C/min, 50 sccm He, 30 min hold at 550 °C) following the MS m/z 17 signal for NH_3 and (b) IPAm-TPD (desorption 200–500 °C, 10 °C/min, 50 sccm He, 30 min hold at 500 °C) following the MS m/z 41 signal for propylene

Figure 2b displays the IPAm-TPD traces of H-ZSM-5-23, H-ZSM-5-50, H-ZSM-5-280 and γ -Al₂O₃. As demonstrated in the figure, the overall intensity of the signals increased in the order γ -Al₂O₃ < H-ZSM-5-280 < H-ZSM-5-50 < H-ZSM-5-23 alike what was observed with the NH₃-TPD traces. The IPAm-TPD traces of all the analyzed materials contained only a single peak centered at approximately 330–340 °C.

Table 1 presents the quantitative total acidity and Brønsted acidity results from the NH₃-TPD and IPAm-TPD analyses along with the Al content determined with XRF for comparison. As shown in Table 1, the amount of both total acid sites and Brønsted acid sites increased in the order γ -Al₂O₃ < H-ZSM-5-280 < H-ZSM-5-50 < H-ZSM-5-23, as expected from the Fig. 2 TPD traces. When comparing the analysis results of the zeolitic samples, Table 1 also shows that the total acidity determined with NH₃-TPD remained higher than the Al content while the Brønsted acidity remained lower than the Al content.

The changes in the acidity of a zeolite before and after the addition of Zn were studied by analyzing H-ZSM-5-50 and Zn/H-ZSM-5-50 with NH₃-TPD and IPAm-TPD. Figure 3a displays the NH₃-TPD traces of H-ZSM-5-50 and Zn/H-ZSM-5-50. As presented in Fig. 3a, both the pristine and the Zn-modified zeolite yielded a trace with a high and a low temperature peak. The high temperature peak maximum shifted from ca. 390 °C to ca. 370 °C and the low temperature peak maximum from ca. 210 °C to ca. 230 °C with the addition of Zn. Furthermore, the high temperature peak on the Zn-modified zeolite was diminished, and the low temperature peak was inflated compared to the unmodified material, and the shape of the high temperature peak appeared wider. The Zn/H-ZSM-5-50 trace contained a strong shoulder at approximately 550 °C coinciding with the start of the isothermal hold at 550 °C, though a shoulder was also less prominently present in the H-ZSM-5-50 trace.

Figure 3b displays the IPAm-TPD traces of H-ZSM-5-50 and Zn/H-ZSM-5-50. In addition to the *m/z* 41 trace associated with propylene produced in the IPAm decomposition, the figure also includes the *m/z* 17 trace associated with the other decomposition product NH₃. Figure 3b figure also includes the *m/z* 44 trace associated with unreacted IPAm, as the fragmentation of IPAm in the MS may produce a *m/z* 41 response that may be confused with the *m/z* 41 response from propylene. When examining the *m/z* 41 traces in Fig. 3b, the H-ZSM-5-50 trace contains a single peak centered at 330 °C and the Zn/H-ZSM-5-50 trace three peaks centered at 335 °C, 400 °C, and 470 °C. Observing the *m/z* 17 trace, the unmodified zeolite yielded a single wide peak while the Zn-modified zeolite trace yielded multiple peaks following the trend of the *m/z* 41 trace. The *m/z* 44 traces of both H-ZSM-5-50 and Zn/H-ZSM-5-50 contained a low

Table 1 The total acidity (A_{tot}) and Brønsted acidity (A_{B}) determined with NH₃-TPD and IPAm-TPD, respectively, with the Al content (C_{Al}) indicated for reference for the zeolitic samples

Sample material	A_{tot} (μmol/g)	A_{B} (μmol/g)	C_{Al} (μmol/g)
H-ZSM-5-23	1696	891	1332
H-ZSM-5-50	695	400	576
Zn/H-ZSM-5-50	697	376	–
H-ZSM-5-280	138	91	120
γ -Al ₂ O ₃	127	45	–

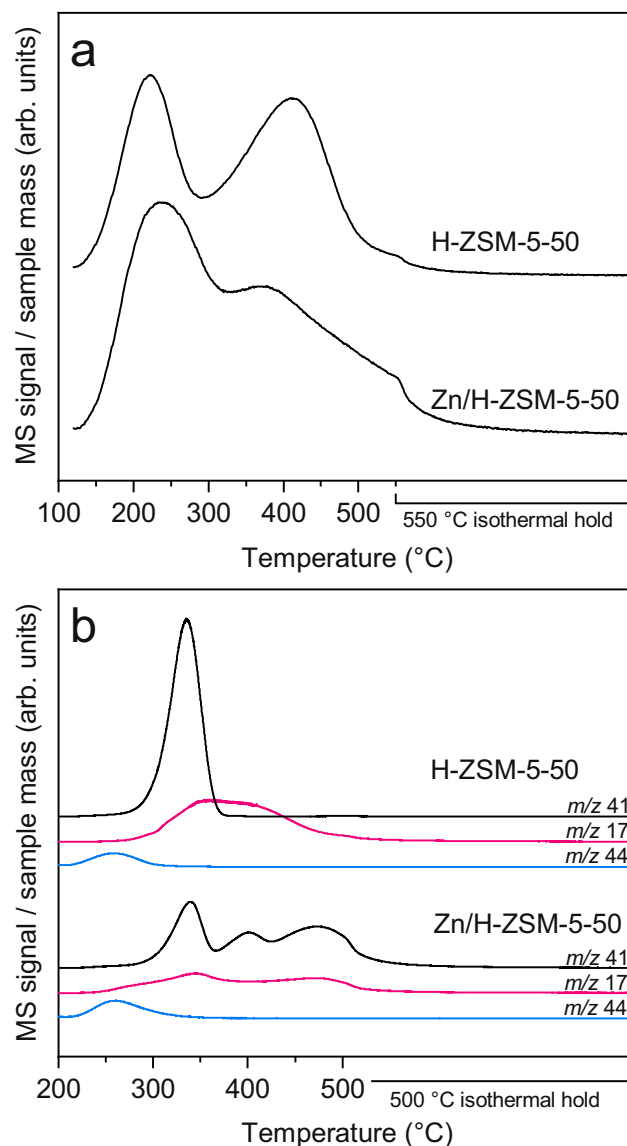


Fig. 3 The desorption traces recorded for H-ZSM-5-50 and Zn/H-ZSM-5-50 during (a) NH₃-TPD (desorption 120–500 °C, 10 °C/min, 50 sccm He, 30 min hold at 550 °C) following the MS *m/z* 17 signal for NH₃ and (b) IPAm-TPD (desorption 200–500 °C, 10 °C/min, 50 sccm He, 30 min hold at 500 °C) following the MS *m/z* 17, 41, and 44 signals for NH₃, propylene, and IPAm, respectively

temperature peak that returned mostly to baseline prior to the main m/z 41 peaks emerging.

Regarding the quantitative acidity results of the H-ZSM-5-50 and Zn/H-ZSM-5-50 samples, the total acidities shown in Table 1 were very similar at 695 $\mu\text{mol/g}$ and 697 $\mu\text{mol/g}$, respectively. The corresponding Brønsted acidities had a minor difference at 400 $\mu\text{mol/g}$ and 376 $\mu\text{mol/g}$, respectively.

Varying the saturation temperature in the temperature-programmed desorption of ammonia.

To examine the effect of the saturation temperature on the analysis results, NH_3 -TPD was performed for a H-ZSM-5-50 sample with the saturation temperatures 50, 100, 120, 150, and 200 °C. Figure 4 displays the NH_3 -TPD traces obtained with the different saturation temperatures. As shown in the figure, the area and appearance of the high temperature peak remained similar between the analyses while the low temperature peak area increased when the saturation temperature was lowered. Moreover, a second low temperature peak appeared when a saturation temperature of 50 °C was used, as shown in Fig. 4.

Table 2 shows the quantitative total acidity results obtained for H-ZSM-5-50 at the different saturation temperatures with each peak quantified separately (see Fig. S1-S5 and Tables S6-S10). As shown in Table 2, the amount of adsorbed NH_3 associated with the highest temperature remained relatively similar regardless of the saturation temperature used. The analysis performed with 50 °C saturation temperature showed a higher amount of adsorbed NH_3 associated with the high temperature peak at 485 $\mu\text{mol/g}$, while the amount for the other analysis runs ranged from 407 $\mu\text{mol/g}$ to 422 $\mu\text{mol/g}$. In turn, the contribution of the low temperature peaks increased when the saturation temperature was lowered and even exceeded the contribution of the high temperature peak with the saturation temperature 50 °C.

4 Discussion

Temperature-programmed desorption results of unmodified zeolites and γ -alumina.

The NH_3 -TPD traces of the unmodified H-ZSM-5-23, H-ZSM-5-50, and H-ZSM-5-280 shown in Fig. 2 appeared typical. The low temperature peaks in the TPD traces were observed at 190–230 °C and the high temperature peaks at 370–430 °C. The peaks fell within the expected low temperature and high temperature peak ranges of 170–280 °C and 370–440 °C [8]. Furthermore, the overall intensity of the measured m/z 17 signals increased expectedly when the theoretical acidity of the material increased. Likewise, the IPAm-TPD traces in Fig. 2 appeared typical. The traces

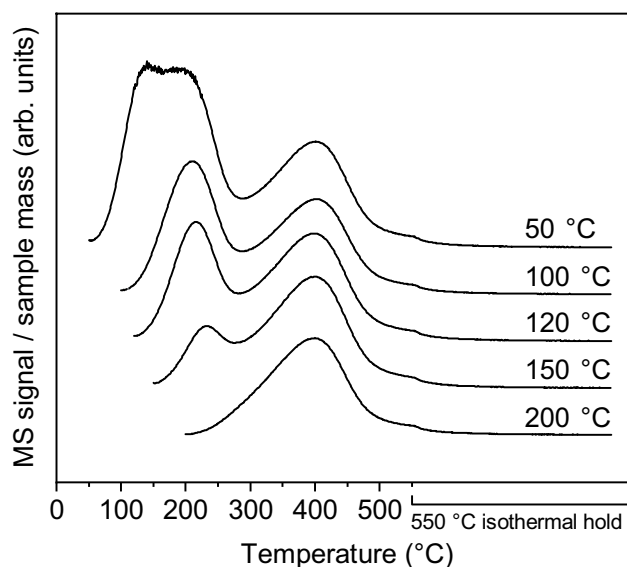


Fig. 4 The NH_3 -TPD desorption traces of H-ZSM-5-50 obtained with a MS (m/z 17) when a saturation temperature of 50, 100, 120, 150, and 200 °C was used (desorption from saturation temperature to 550 °C, 10 °C/min, 50 sccm He, 30 min hold at 550 °C)

Table 2 Perceived total acidity (amount of adsorbed NH_3) (A_{tot}) of H-ZSM-5-50 when the saturation temperatures of 50, 100, 120, 150, and 200 °C were used

Saturation temperature (°C)	A_{tot} ($\mu\text{mol/g}$)			Sum
	Peak 1 (approx. 100 °C)	Peak 2 (approx. 200 °C)	Peak 3 (approx. 400 °C)	
50	237	565	485	1260
100	–	370	411	782
120	–	243	407	650
150	–	117	411	528
200	–	–	422	422

contained each a single m/z 41 peak within the typical temperature range of 300–375 °C [17]. As with the NH_3 -TPD traces, the overall intensity of the measured m/z 41 signals increased with the theoretical acidity.

A γ - Al_2O_3 sample was also analyzed for reference. The sample yielded a single peak in both NH_3 -TPD and IPAm-TPD and exhibited some total acidity but minimal Brønsted acidity according to the quantitative NH_3 -TPD and IPAm-TPD results in Table 1. The results were consistent with established views on γ - Al_2O_3 acidity, as the material is considered primarily Lewis acidic [47], while some Brønsted acidic sites may be present due to the hydration and hydroxylation of the surface [48].

Comparing the quantitative acidity results of the unmodified zeolites shown in Table 1 to values available in literature, the observed total acidity of H-ZSM-5-23, H-ZSM-5-50, and H-ZSM-5-280 in Table 1 appeared high. For example, total acidity values of up to 1464 $\mu\text{mol/g}$ [28] could be found for commercial H-ZSM-5-23 in literature, and the

value 1696 $\mu\text{mol/g}$ observed in this work exceeded it. The observed Brønsted acidity of the materials appeared more intermediate to values reported by others. For example, the Brønsted acidity of commercial H-ZSM-5-23 was 891 $\mu\text{mol/g}$ in this work, while a values of 435–1260 $\mu\text{mol/g}$ have been reported for H-ZSM-5 materials with $\text{SiO}_2/\text{Al}_2\text{O}_3$ ratios of 23–25 [35, 38, 39]. As stated previously, the quantitative acidity results may be influenced by the analysis conditions [18]. Ideally analysis results intended for comparison should be performed in the same conditions, and differences in them may explain the observed differences in quantitative results.

To provide a comparison point less susceptible to influences from the analysis conditions, the Al content of the zeolites was used to estimate the theoretical acidity of the unmodified H-ZSM-5-23, H-ZSM-5-50, and H-ZSM-5-280 samples and used as a comparison point for the quantitative acidity results. To better illustrate the relation of the zeolite sample total acidity and Brønsted acidity to the Al content, Fig. 5 displays the observed total and Brønsted acidity of H-ZSM-5-23, H-ZSM-5-50, and H-ZSM-5-280 plotted against the Al content of the materials obtained with XRF. The diagonal in Fig. 5 indicates an idealized case where acidic sites would occur in a 1:1 ratio with Al atoms in the zeolite.

As demonstrated in Fig. 5, both the total and Brønsted acidity appeared to show a linear correlation with the Al content. The coefficient of determination R^2 was close to 1 for both fits indicating that the results of both NH_3 -TPD and IPAm-TPD were proportional to the amount of theoretical acid sites in the analyzed zeolites. The NH_3 -TPD and IPAm-TPD results deviated from the theoretical 1:1 ratio of acid sites to Al by a constant of approximately 1.26 and 0.67, respectively.

Observing a lower Brønsted acidity than estimated with the Al content appears logical. Estimating theoretical acidity with XRF-based Al content assumes that all the Al is associated with the framework, as Brønsted sites are mostly associated with framework Al. In reality, zeolite materials also contain extra-framework Al. Consequently, each Al atom observed with XRF may not be associated with a Brønsted acid site, and the Brønsted acid sites amount determined with IPAm-TPD is often less than the amount of Al in the material [49]. As a further note, some uncertainty to the estimate of theoretical acidity is introduced by the standardless Omnic quantification method used to determine the Al content. A more accurate result for the Al content could be achieved with a quantification method based on standards, though the amount of framework Al could also be selectively determined with ^{27}Al nuclear magnetic resonance spectroscopy [1].

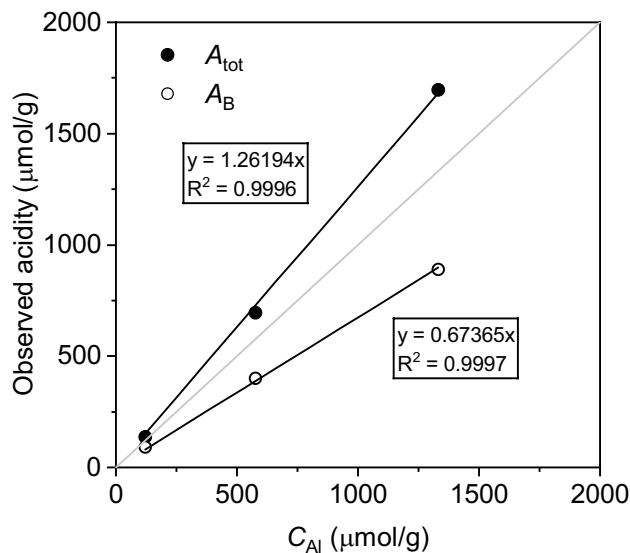


Fig. 5 Linear fits to the quantity of total and Brønsted acid sites on H-ZSM-5-280, H-ZSM-5-50, and H-ZSM-5-23 as observed with NH_3 - and IPAm-TPD, respectively, and the Al content of the materials. The intercepts of the linear fits were fixed at 0

The observed amount of Brønsted sites could also decrease if the propylene and NH_3 were reacting back to propylamine (PAm). In such case, the Brønsted acidity could have been underestimated as only the propylene-related m/z 41 signal was used to quantify the Brønsted acidity. Indeed, NH_3 has been observed to aminate lower alkenes in elevated temperatures [50]. However, the reaction is exothermic and the amount of propylene and NH_3 reacting back to PAm would decrease in high temperatures [51]. Moreover, it's likely that a small m/z 44 response would be observed if any amination occurred in the analysis conditions. According to the data in Fig. 3b, no PAm was detected in higher temperatures, as only a m/z 41 and m/z 17 response was observed above approximately 300 °C. Therefore, the amination of propylene is unlikely to have affected the quantitative results.

Compared to the trend in Brønsted acidity, observing a higher total acidity than what was estimated with the Al content was more unexpected. Though the extra-framework Al atoms could give rise to Lewis sites, some extra-framework Al species cannot be considered acidic [52]. The NH_3 -TPD and IPAm-TPD analysis conditions of this work followed the instrument manufacturer recommendations and were similar to conditions reported in literature. Significantly, a different saturation temperature was recommended for NH_3 -TPD and IPAm-TPD analyses and consequently used in this work. The saturation temperature affects the probe molecule surface coverage, and as adsorption is typically exothermic, a higher coverage would be expected at a lower temperature [53]. As the NH_3 -TPD saturation temperature used was lower than the IPAm-TPD saturation temperature,

the results for the total acidity could have been higher than for the Brønsted acidity due to the analysis conditions.

Experiments varying the saturation temperature showed that the contribution of the low temperature peak to the total amount of adsorbed NH_3 varied with the temperature used, while the amount of NH_3 associated with the high temperature peak generally remained similar regardless of the saturation temperature. Only the analysis with 50 °C saturation temperature showed a slightly higher amount of adsorbed NH_3 associated with the high temperature peak at 485 $\mu\text{mol/g}$.

The increase in adsorbed NH_3 with low saturation temperatures has been previously explained by NH_3 hydrogen bonding. Lónyi and Valyon [42] studied NH_3 adsorption on H-ZSM-5 at 25, 100, 150, 250, and 350 °C. They found that the adsorbed NH_4^+ species formed hydrogen bonds with additional NH_3 molecules during NH_3 -TPD [42]. The hydrogen bonds were observed to be stable even at elevated temperatures, and appeared to contribute to the low temperature peak of the NH_3 -TPD trace [42]. The NH_3 -TPD traces of this work with the selected saturation temperatures showed similar trends to the traces obtained by Lónyi and Valyon [42]. This could indicate that the perceived total acidity obtained with the NH_3 -TPD method using a 120 °C saturation temperature was inflated by the multilayer adsorption of NH_3 .

Effect of zinc modification on observed acidity.

The quantitative results of the H-ZSM-5-50 and Zn/H-ZSM-5-50 showed little differences. The total acidity determined with NH_3 -TPD was 695 $\mu\text{mol/g}$ and 697 $\mu\text{mol/g}$ H-ZSM-5-50 and Zn/H-ZSM-5-50, respectively. The Brønsted acidity values obtained with IPAm-TPD had more of a difference were 400 $\mu\text{mol/g}$ and 376 $\mu\text{mol/g}$ for H-ZSM-5-50 and Zn/H-ZSM-5-50, respectively. The relative standard deviation of the NH_3 -TPD and IPAm-TPD results was found to be approximately 4% in repeat experiments with H-ZSM-5-50 (Table S4, Table S5). Consequently, the observed quantity of acidic sites obtained with both NH_3 -TPD and IPAm-TPD could be concluded to have remained the same despite the Zn-modification. In particular, the Brønsted acidity of the Zn-modified material was expected to change, as typically the introduction of Zn increases the Lewis acidity and decreases the Brønsted acidity. For example, Gong et al. [54] observed a significant increase in Lewis acidity as well as a decrease in Brønsted acidity with adsorbed pyridine characterization by infrared spectroscopy for a Zn/H-ZSM-5-25 material prepared with ALD.

Despite the quantitative NH_3 -TPD and IPAm-TPD results of H-ZSM-5-50 and Zn/H-ZSM-5-50 remaining similar, the TPD traces obtained with both methods presented some differences. In the NH_3 -TPD traces, the magnitudes of the peaks changed, and the low temperature peak

and high temperature peaks shifted by approximately 20 °C with the addition of Zn. The observed shift could be possibly due to the combination of a change in the magnitude of the peaks and NH_3 re-adsorption to the sample, as the low temperature peak with increased magnitude shifted to a higher temperature and the high temperature peak with decreased magnitude shifted to a lower temperature. The decrease of magnitude in the high temperature peak and the increase in the low temperature peak suggest a decrease in strong acid sites and an increase in weak acid sites.

While the differences between the NH_3 -TPD traces were moderate, the IPAm-TPD traces showed major differences between the pristine and Zn-modified H-ZSM-5-50. The m/z 41 traces of both H-ZSM-5-50 and Zn/H-ZSM-5-50 were expected to have a single peak, as the IPAm decomposition should occur at a similar temperature regardless of the acid site strength [17]. Despite the result being unexpected, precedents of multiple peaks observed in IPAm-TPD for Zn-containing zeolitic samples are available in literature. For instance, Tamiyakul et al. [39] performed IPAm-TPD of Zn/H-ZSM-5 with various Zn loadings and observed m/z 41 peaks at approximately 350 °C, 390 °C, and 480 °C for the tested materials [39]. The m/z 41 peaks in Fig. 3b were observed at similar temperatures at approximately 335 °C, 400 °C, and 470 °C. The additional peaks were suggested to be induced by water contaminants in the IPAm used for the TPD analysis, which was claimed to regenerate Brønsted sites at high temperatures [39].

The regeneration of Brønsted sites could explain the unexpected shape of the IPAm-TPD trace as well as the seemingly inflated result for Brønsted acidity. However, observing additional m/z 41 peaks originating from regenerated Brønsted sites would require the retention of unreacted IPAm in the sample. The current understanding is that any IPAm adsorbed to weaker sites exits the sample prior to the decomposition reaction [16, 18, 23]. According to the m/z 44 data in Fig. 3b, the unreacted IPAm appeared to mostly exit the sample prior to the main decomposition peaks at approximately 200–325 °C. This would eliminate the possibility of further IPAm decomposing on regenerated Brønsted sites.

The unusual shape of the Zn/H-ZSM-5-50 IPAm-TPD trace could have other explanations that do not address the quantitative results being higher than expected. For example, isolated Zn^{2+} sites have been observed to interact with propylene [55]. Interaction that would delay the release of propylene could yield a IPAm trace with multiple peaks. Nevertheless, the NH_3 -related m/z 17 trace showed similar trends to the propylene-related m/z 41 peaks, which would indicate some IPAm decomposition occurring at a higher temperature and not just the detection of propylene being delayed.

In addition to the IPAm-TPD trace being altered by the presence of Zn, also the NH₃-TPD trace of the Zn-modified H-ZSM-5-50 showed some changes. It could be speculated that the interaction between the probe molecules and the sample material is altered by the introduction of Lewis sites in the Zn-modification, which is particularly noticeable in the IPAm-TPD analysis. A study by Kanazirev et al. [56] observed significant changes in the interaction of *n*-propylamine and Ga- and In-modified H-MFI in TPD analyses. The authors observed the release of NH₃ at an unusually low temperature during the heating program, a shift in the temperature at which propylene is released, as well as propionitrile species being present in the gas flow downstream the sample cell [56]. The decomposition mode of the amine was suggested to have been altered due to the formation of complexes between Lewis acidic Ga and In cations and *n*-propylamine [56].

Furthermore, Lewis acid sites have been suggested to sever the C—N bond. Sokoll et al. [57] investigated the adsorption of IPAm on various oxides with TPD and infrared spectroscopy (IR). The authors observed some IPAm decomposition on γ -Al₂O₃ and proposed a mechanism for the decomposition on the Lewis acidic sites [57]. They also observed the formation of acetonitrile and methane in high temperatures consistent with another surface reaction for IPAm besides the formation of propylene and NH₃ [57]. No further studies appeared to discuss the C—N bond scission in amine-TPD caused by Lewis acid sites.

Only a few studies appeared to examine the interaction between IPAm and sample materials containing both Lewis and Brønsted sites. Further work could be conducted to explain the IPAm-TPD results of Zn-modified zeolites more comprehensively. Such work would improve the understanding of IPAm-TPD applicability as an analysis method for the surface acidity of materials with multiple types of acidic sites.

5 Conclusions

This work aimed to present a comparison of NH₃-TPD and IPAm-TPD as analysis methods for the acidity of zeolitic samples. To compare the analysis results obtained with both methods, NH₃-TPD and IPAm-TPD were performed for selected unmodified zeolites, a Zn-modified zeolite, and a γ -Al₂O₃ reference sample. Additionally, to further examine the observed trends, NH₃-TPD measurements were performed at selected saturation temperatures for H-ZSM-5-50.

The NH₃-TPD and IPAm-TPD analyses yielded typical traces for H-ZSM-5-23, H-ZSM-5-50, and H-ZSM-5-280, indicating that the methods were successfully applied in the study. Further supporting this conclusion, the quantitative

acidity results of the γ -Al₂O₃ reference sample exhibited some acidity in NH₃-TPD but only minor Brønsted acidity in IPAm-TPD, consistent with the current understanding of γ -Al₂O₃ surface chemical properties. The quantitative acidity results for the unmodified zeolites obtained in the chosen analysis conditions appeared relatively high for both total acidity and Brønsted acidity when compared to literature values. When compared to the theoretical acidity of the zeolites estimated with the XRF-based Al content, the results of the NH₃-TPD method were systematically higher whereas the IPAm-TPD results were systematically lower. Still, both results showed a linear correlation to the Al content indicating that the NH₃-TPD and IPAm-TPD results were proportional to the theoretical amount of acid sites in the zeolites.

In this work, the quantitative NH₃-TPD and IPAm-TPD results remained similar for H-ZSM-5-50 and Zn/H-ZSM-5-50 despite Zn-modification. However, differences were observed in the appearance of both the NH₃-TPD and IPAm-TPD traces with significant differences observed in the IPAm-TPD trace, suggesting a difference in surface chemical properties. The results agreed with reports of a potential change in the interaction of IPAm and oxide sample materials with the presence of Lewis acid sites available in literature. The interaction could be investigated further to provide a more comprehensive understanding of the IPAm-TPD results of Zn-modified zeolites and the applicability of IPAm-TPD for the analysis surface acidity when multiple types of acidic sites are present.

Supplementary Information The online version contains supplementary material available at <https://doi.org/10.1007/s11244-025-02112-0>.

Acknowledgements This work was funded by Business Finland (GreenAro project) and made use of the Aalto University Bioeconomy and RawMatters research infrastructures. Christine Gonsalves is acknowledged for performing the ALD of Zn on H-ZSM-5-50.

Funding Open Access funding provided by Aalto University.

Declarations

Competing Interests The authors have no competing interests to declare that are relevant to the content of this article.

Open Access This article is licensed under a Creative Commons Attribution 4.0 International License, which permits use, sharing, adaptation, distribution and reproduction in any medium or format, as long as you give appropriate credit to the original author(s) and the source, provide a link to the Creative Commons licence, and indicate if changes were made. The images or other third party material in this article are included in the article's Creative Commons licence, unless indicated otherwise in a credit line to the material. If material is not included in the article's Creative Commons licence and your intended use is not permitted by statutory regulation or exceeds the permitted use, you will need to obtain permission directly from the copyright

holder. To view a copy of this licence, visit <http://creativecommons.org/licenses/by/4.0/>.

References

- Derouane EG, Védrine JC, Pinto RR et al (2013) The acidity of zeolites: concepts, measurements and relation to catalysis: A review on experimental and theoretical methods for the study of zeolite acidity. *Catal Rev* 55:454–515. <https://doi.org/10.1080/01614940.2013.822266>
- Järvinen E (2024) Acidity characterisation of zeolites for glycerol aromatisation with temperature-programmed desorption. Aalto University
- Góra-Marek K, Melián-Cabrera I (2021) A note on the acid strength of porous materials assessed by thermal methods. *Microporous Mesoporous Mater* 310:110638. <https://doi.org/10.1016/j.micromeso.2020.110638>
- Al-Dughaiter AS, de Lasa H (2014) HZSM-5 zeolites with different SiO₂/Al₂O₃ ratios. Characterization and NH₃ desorption kinetics. *Ind Eng Chem Res* 53:15303–15316. <https://doi.org/10.1021/ie4039532>
- Benaliouche F, Boucheffa Y, Ayrault P et al (2008) NH₃-TPD and FTIR spectroscopy of pyridine adsorption studies for characterization of Ag- and Cu-exchanged X zeolites. *Microporous Mesoporous Mater* 111:80–88. <https://doi.org/10.1016/j.micromeso.2007.07.006>
- Liu D, Yuan P, Liu H et al (2013) Quantitative characterization of the solid acidity of montmorillonite using combined FTIR and TPD based on the NH₃ adsorption system. *Appl Clay Sci* 80–81:407–412. <https://doi.org/10.1016/j.clay.2013.07.006>
- Hunger B, Heuchel M, Clark LA, Snurr RQ (2002) Characterization of acidic OH groups in zeolites of different types: an interpretation of NH₃-TPD results in the light of confinement effects. *J Phys Chem B* 106:3882–3889. <https://doi.org/10.1021/jp012688n>
- Rodríguez-González L, Hermes F, Bertmer M et al (2007) The acid properties of H-ZSM-5 as studied by NH₃-TPD and 27Al-MAS-NMR spectroscopy. *Appl Catal Gen* 328:174–182. <https://doi.org/10.1016/j.apcata.2007.06.003>
- Bagnasco G (1996) Improving the selectivity of NH₃TPD measurements. *J Catal* 159:249–252. <https://doi.org/10.1006/jcat.1996.0085>
- Martins GVA, Berlier G, Bisio C et al (2008) Quantification of Brønsted acid sites in microporous catalysts by a combined FTIR and NH₃-TPD study. *J Phys Chem C* 112:7193–7200. <https://doi.org/10.1021/jp710613q>
- Post JG, van Hooff JHC (1984) Acidity And activity of H-ZSM—5 measured with NH₃-t.p.d. And n-hexane cracking. *Zeolites* 4:9–14. [https://doi.org/10.1016/0144-2449\(84\)90065-4](https://doi.org/10.1016/0144-2449(84)90065-4)
- Pinto RR, Borges P, Lemos MANDA et al (2005) Correlating NH₃-TPD and 1H MAS NMR measurements of zeolite acidity: proposal of an acidity scale. *Appl Catal Gen* 284:39–46. <https://doi.org/10.1016/j.apcata.2005.01.021>
- ASTM International (2024) Standard test method for determination of catalyst acidity by Ammonia chemisorption. ASTM D4824-24. <https://doi.org/10.1520/D4824-24>
- Abdelrahman OA, Altman EI, Cargnello M et al (2024) A career in catalysis: Raymond J. Gorte. *ACS Catal* 14:12895–12916. <https://doi.org/10.1021/acscatal.4c02998>
- Kofke TJG, Gorte RJ, Farneth WE (1988) Stoichiometric adsorption complexes in H-ZSM-5. *J Catal* 114:34–45. [https://doi.org/10.1016/0021-9517\(88\)90006-1](https://doi.org/10.1016/0021-9517(88)90006-1)
- Parrillo DJ, Adamo AT, Kokotailo GT, Gorte RJ (1990) Amine adsorption in H-ZSM-5. *Appl Catal* 67:107–118. [https://doi.org/10.1016/S0166-9834\(00\)84435-8](https://doi.org/10.1016/S0166-9834(00)84435-8)
- Tittensor JG, Gorte RJ, Chapman DM (1992) Isopropylamine adsorption for the characterization of acid sites in silica-alumina catalysts. *J Catal* 138:714–720. [https://doi.org/10.1016/0021-9517\(92\)90318-C](https://doi.org/10.1016/0021-9517(92)90318-C)
- Gorte RJ (1996) Temperature-programmed desorption for the characterization of oxide catalysts. *Catal Today* 28:405–414. [https://doi.org/10.1016/S0920-5861\(96\)00249-0](https://doi.org/10.1016/S0920-5861(96)00249-0)
- Gorte RJ, White D (1997) Interactions of chemical species with acid sites in zeolites. *Top Catal* 4:57–69. <https://doi.org/10.1023/A:1019167601251>
- Gorte RJ, Kokotailo GT, Biaglow AI et al (1991) A study of acid sites in substituted Aipo-5. In: Jacobs PA, Jaeger NI, Kubelková L, Wichterlov' B (eds) *Studies in surface science and catalysis*. Elsevier, pp 181–187
- Biaglow AI, Gittleman C, Gorte RJ, Madon RJ (1991) 2-Propanamine adsorption on a fluid catalytic cracking catalyst. *J Catal* 129:88–93. [https://doi.org/10.1016/0021-9517\(91\)90011-R](https://doi.org/10.1016/0021-9517(91)90011-R)
- Biaglow AI, Adamo AT, Kokotailo GT, Gorte RJ (1991) An examination of the acid sites in SAPO-5. *J Catal* 131:252–259. [https://doi.org/10.1016/0021-9517\(91\)90342-2](https://doi.org/10.1016/0021-9517(91)90342-2)
- Parrillo DJ, Gorte RJ (1992) Characterization of stoichiometric adsorption complexes in H-ZSM-5 using microcalorimetry. *Catal Lett* 16:17–25. <https://doi.org/10.1007/BF00764350>
- Pereira C, Gorte RJ (1992) Method for distinguishing Brønsted-acid sites in mixtures of H-ZSM-5, H-Y and silica-alumina. *Appl Catal Gen* 90:145–157. [https://doi.org/10.1016/0926-860X\(92\)85054-F](https://doi.org/10.1016/0926-860X(92)85054-F)
- Web of Science query results for NH₃-TPD <https://www.webofscience.com/wos/woscc/summary/016f61ee-84f7-4d0f-a3a9-0064915fcf71-0119d602be/date-descending/1>. Accessed 29 Oct 2024
- Web of Science query results for IPAm-TPD <https://www.webofscience.com/wos/woscc/summary/bdfa6267-96a5-46c0-8c36-699d1700976d-01172c2d03/date-descending/1>. Accessed 29 Oct 2024
- Trachta M, Bludský O, Vaculík J et al (2023) Investigation of Brønsted acidity in zeolites through adsorbates with diverse proton affinities. *Sci Rep* 13:12380. <https://doi.org/10.1038/s41598-023-39667-5>
- He S, Zuur K, Santosa DS et al (2021) Catalytic conversion of pure glycerol over an un-modified H-ZSM-5 zeolite to bio-based aromatics. *Appl Catal B Environ* 281:119467. <https://doi.org/10.1016/j.apcatb.2020.119467>
- Le TT, Qin W, Agarwal A et al (2023) Elemental zoning enhances mass transport in zeolite catalysts for methanol to hydrocarbons. *Nat Catal* 6:254–265. <https://doi.org/10.1038/s41929-023-00927-2>
- Choi S-W, Kim W-G, So J-S et al (2017) Propane dehydrogenation catalyzed by gallosilicate MFI zeolites with perturbed acidity. *J Catal* 345:113–123. <https://doi.org/10.1016/j.jcat.2016.11.017>
- Björger M, Joensen F, Spangsborg Holm M et al (2008) Methanol to gasoline over zeolite H-ZSM-5: improved catalyst performance by treatment with NaOH. *Appl Catal Gen* 345:43–50. <https://doi.org/10.1016/j.apcata.2008.04.020>
- Phung TK, Radikapatama R, Garbarino G et al (2015) Tuning of product selectivity in the conversion of ethanol to hydrocarbons over H-ZSM-5 based zeolite catalysts. *Fuel Process Technol* 137:290–297. <https://doi.org/10.1016/j.fuproc.2015.03.012>
- Zhu X, Lobban LL, Mallinson RG, Resasco DE (2010) Tailoring the mesopore structure of HZSM-5 to control product distribution in the conversion of Propanal. *J Catal* 271:88–98. <https://doi.org/10.1016/j.jcat.2010.02.004>

34. Kim YT, Jung K-D, Park ED (2011) A comparative study for gas-phase dehydration of glycerol over H-zeolites. *Appl Catal Gen* 393:275–287. <https://doi.org/10.1016/j.apcata.2010.12.007>
35. You SJ, Park ED (2014) Effects of dealumination and desilication of H-ZSM-5 on xylose dehydration. *Microporous Mesoporous Mater* 186:121–129. <https://doi.org/10.1016/j.micromeso.2013.11.042>
36. Lew CM, Chen C-Y, Long GJ et al (2022) Synthesis, physico-chemical characterization, and catalytic evaluation of Fe³⁺-Containing SSZ-70 zeolite. *ACS Catal* 12:6464–6477. <https://doi.org/10.1021/acscatal.2c01361>
37. Manrique C, Guzmán A, Solano R, Echavarría A (2019) Phosphorous-Modified Beta zeolite and its performance in vacuum gas oil hydrocracking activity. *Energy Fuels* 33:3483–3491. <https://doi.org/10.1021/acs.energyfuels.8b04485>
38. Peters TA, Benes NE, Holmen A, Keurentjes JTF (2006) Comparison of commercial solid acid catalysts for the esterification of acetic acid with butanol. *Appl Catal Gen* 297:182–188. <https://doi.org/10.1016/j.apcata.2005.09.006>
39. Tamiyakul S, Anutamjarikun S, Jongpatiwut S (2016) The effect of Ga and Zn over HZSM-5 on the transformation of palm fatty acid distillate (PFAD) to aromatics. *Catal Commun* 74:49–54. <https://doi.org/10.1016/j.catcom.2015.11.002>
40. Characterization of Acid Sites Using Temperature-Programmed Desorption (2025) In: *Micromeritics*. Accessed 12 Mar 2025 <https://micromeritics.com/resources/characterization-of-acid-sites-using-temperature-programmed-desorption/>
41. Acid Site Characterization of H⁺ ZSM-5 (2025) (SiO₂/Al₂O₃:30/1): A Pulse Chemisorption and TPD Application for the AutoChem. In: *Micromeritics*. Accessed 12 Mar 2025 <https://micromeritics.com/resources/acid-site-characterization-of-h-zsm-5-sio2-al2o3-30-1-a-pulse-chemisorption-and-tpd-application-for-the-autochem/>
42. Lónyi F, Valyon J (2001) On the interpretation of the NH₃-TPD patterns of H-ZSM-5 and H-mordenite. *Microporous Mesoporous Mater* 47:293–301. [https://doi.org/10.1016/S1387-1811\(01\)00389-4](https://doi.org/10.1016/S1387-1811(01)00389-4)
43. Farneth WE, Gorte RJ (1995) Methods for characterizing zeolite acidity. *Chem Rev* 95:615–635. <https://doi.org/10.1021/cr00035a007>
44. Miyamoto T, Katada N, Kim J-H, Niwa M (1998) Acidic property of MFI-Type gallosilicate determined by Temperature-Programmed desorption of Ammonia. *J Phys Chem B* 102:6738–6745. <https://doi.org/10.1021/jp980007r>
45. Yim J, Haimi E, Mäntymäki M, Kärkäs V, Bes R, Arandia Gutierrez A, Meinander K, Brünner P, Grehl T, Gell L, Viinikainen T, Honkala K, Huotari S, Karinen R, Putkonen M, Puurunen RL (2023) Atomic Layer Deposition of Zinc Oxide on Mesoporous Zirconia Using Zinc(II) Acetylacetonate and Air. *Chem Mater* 35:7915–7930. <https://doi.org/10.1021/acs.chemmater.3c00668>
46. Bielecka K, Kurtek W, Banás D et al X-ray Diffraction and Elemental Analysis of Medical and Environmental Samples. In: *Proceedings of the XLVIIIth Zakopane School of Physics*. Acta Physica Polonica A, Zakopane, Poland, pp 911–918
47. Pines H, Haag WO (1960) Alumina: catalyst and support. I. Alumina, its intrinsic acidity and catalytic Activity. *J Am Chem Soc* 82:2471–2483. <https://doi.org/10.1021/ja01495a021>
48. Christiansen MA, Mpourmpakis G, Vlachos DG (2013) Density functional Theory-Computed mechanisms of ethylene and diethyl ether formation from ethanol on γ -Al₂O₃(100). *ACS Catal* 3:1965–1975. <https://doi.org/10.1021/cs4002833>
49. Gorte RJ (1999) What do we know about the acidity of solid acids? *Catal Lett* 62:1–13. <https://doi.org/10.1023/A:1019010013989>
50. Mizuno N, Tabata M, Uematsu T, Iwamoto M (1994) 1.8 Direct amination of lower alkenes with Ammonia over zeolite catalysts. In: Hattori H, Misono M, Ono Y (eds) *Studies in surface science and catalysis*. Elsevier, pp 71–76
51. Lequitte M, Figueras F, Moreau C, Hub S (1996) Amination of Butenes over protonic zeolites. *J Catal* 163:255–261. <https://doi.org/10.1006/jcat.1996.0326>
52. Ravi M, Sushkevich VL, van Bokhoven JA (2020) Towards a better Understanding of Lewis acidic aluminium in zeolites. *Nat Mater* 19:1047–1056. <https://doi.org/10.1038/s41563-020-0751-3>
53. Bastos-Neto M, de Azevedo DCS, de Lucena SMP (2020) Adsorption. In: *Kirk-Othmer encyclopedia of chemical technology*. Wiley, Ltd, pp 1–59
54. Gong T, Qin L, Lu J, Feng H (2015) ZnO modified ZSM-5 and Y zeolites fabricated by atomic layer deposition for propane conversion. *Phys Chem Chem Phys* 18:601–614. <https://doi.org/10.1039/C5CP05043J>
55. Camacho-Bunquin J, Aich P, Ferrandon M et al (2017) Single-site zinc on silica catalysts for propylene hydrogenation and propane dehydrogenation: synthesis and reactivity evaluation using an integrated atomic layer deposition-catalysis instrument. *J Catal* 345:170–182. <https://doi.org/10.1016/j.jcat.2016.10.017>
56. Kanazirev V, Price GL, Dooley KM (1994) Change in the decomposition mode of 1-propanamine due to the presence of cations in MFI zeolite. *Catal Lett* 24:227–233. <https://doi.org/10.1007/BF00811795>
57. Sokoll R, Hobert H, Schmuck I (1990) Thermal desorption and infrared studies of amines adsorbed on SiO₂, Al₂O₃, Fe₂O₃, MgO, and CaO II. Isopropylamine and cyclohexylamine. *J Catal* 125:276–284. [https://doi.org/10.1016/0021-9517\(90\)90303-2](https://doi.org/10.1016/0021-9517(90)90303-2)

Publisher's Note Springer Nature remains neutral with regard to jurisdictional claims in published maps and institutional affiliations.